Accessing Sodium Ferrate Complexes Containing Neutral and Anionic N-Heterocyclic Carbene Ligands: Structural, Synthetic, and Magnetic Insights

ARTICLE *in* INORGANIC CHEMISTRY · SEPTEMBER 2015

Impact Factor: 4.76 · DOI: 10.1021/acs.inorgchem.5b01638 · Source: PubMed

6 AUTHORS, INCLUDING:

Thomas Cadenbach

Escuela Politécnica Nacional

44 PUBLICATIONS **643** CITATIONS

SEE PROFILE

Alan R. Kennedy

University of Strathclyde

550 PUBLICATIONS **6,937** CITATIONS

SEE PROFILE

Ivana Borilovic

University of Barcelona

8 PUBLICATIONS **6** CITATIONS

SEE PROFILE

Inorganic Chemistry

Article

pubs.acs.org/IC

Accessing Sodium Ferrate Complexes Containing Neutral and Anionic N-Heterocyclic Carbene Ligands: Structural, Synthetic, and Magnetic Insights

Lewis C. H. Maddock,[†] Thomas Cadenbach,[†] Alan R. Kennedy,[†] Ivana Borilovic,[‡] Guillem Aromí,[‡] and Eva Hevia*[,†]

[†]WestCHEM, Department of Pure and Applied Chemistry, University of Strathclyde, 295 Cathedral Street, Glasgow, U.K. G1 1XL

[‡]Departament de Química Inorgànica, Universitat de Barcelona, Diagonal 645, 08028 Barcelona, Spain

Supporting Information

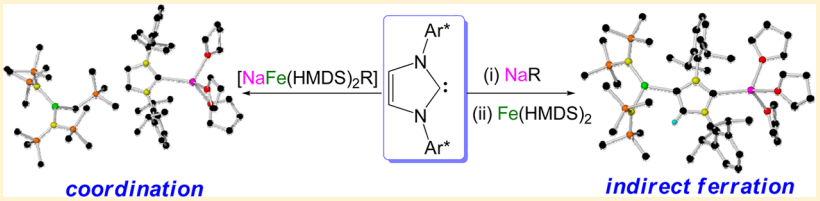

ABSTRACT: This study reports the synthesis and single-crystal X-ray crystallographic, NMR spectroscopic, and magnetic characterization of a series of sodium ferrates using bis(amide) $Fe(HMDS)_2$ as a precursor (HMDS = 1,1,1,3,3,3-hexamethyldisilazide). Reaction with sodium reagents NaHMDS and $NaCH_2SiMe_3$ in hexane afforded donor-solvent-free sodium ferrates $[\{NaFe(HMDS)_3\}_\infty]$ (**1**) and $[\{NaFe(HMDS)_2(CH_2SiMe_3)\}_\infty]$ (**2**), respectively, which exhibit contacted ion pair structures, giving rise to new polymeric chain arrangements made up of a combination of inter- and intramolecular Na···Me(HMDS) electrostatic interactions. Addition of the unsaturated NHC **IPr** (**IPr** = 1,3-bis(2,6-diisopropylphenyl)imidazol-2-ylidene) to **1** and **2** caused deaggregation of their polymeric structures to form discrete NHC-stabilized solvent-separated ion pairs $[Na(IPr)_2]^+[Fe(HMDS)_3]^-$ (**3**) and $[(THF)_3{\cdot}NaIPr]^+[Fe(HMDS)_2CH_2SiMe_3]^-$ (**4**), where in both cases, the NHC ligand coordinates preferentially to Na. In contrast, when **IPr** is sequentially reacted with the single-metal reagents $NaCH_2SiMe_3$ and $Fe(HMDS)_2$, the novel heteroleptic ferrate $(THF)_3Na[:C\{[N(2,6\text{-}^iPr_2C_6H_3)]_2CHCFe(HMDS)_2\}]$ (**5**) is obtained. This contains an anionic NHC ligand acting as an unsymmetrical bridge between the two metals, coordinating through its abnormal C4 position to Fe and its normal C2 position to Na. The formation of **5** can be described as an indirect ferration process where IPr is first metalated at the C4 position by the polar sodium alkyl reagent, which in turn undergoes transmetalation to the more electronegative $Fe(HMDS)_2$ fragment. Treatment of **5** with 1 molar equiv of methyl triflate (MeOTf) led to the isolation and structural elucidation of the neutral abnormal NHC (aNHC) tricoordinate iron complex $[CH_3C\{[N(2,6\text{-}iPr_2C_6H_3)]_2CHCFe(HMDS)_2\}]$ (**6**) with the subsequent elimination of NaOTf, disclosing the selectivity of complex **5** to react with this electrophile via its C2 position, leaving its Fe−C4 and Fe−N bonds intact. The magnetic susceptibility properties of compounds **1**−**6** have been examined. This study revealed a drastic change of magnetic susceptibility in replacing a pure σ donor from an idealized trigonal coordination environment by an NHC π donating character.

INTRODUCTION

Over the past decade the chemistry of s-block heterobimetallic (ate) reagents, which combine metals of markedly different polarities, has developed at a remarkable pace, with the realization of their synergic chemical profiles, which cannot be replicated by their single-metal components.[1] When cooperative effects are switched on, these ates, usually made by pairing an alkali metal with either Mg or Zn, can display enhanced reactivities, unique selectivities, and superior functional group tolerance to traditional polar organometallic reagents such as organolithium and Grignard reagents.[2] Finding widespread applications in a myriad of organic transformations, some of these multicomponent systems have emerged as versatile and potent deprotonating reagents, allowing direct magnesiation or zincation of a wide range of aromatic substrates.[3] Isolation of key organometallic intermediates involved in these transformations has provided new insights into how these bimetallic systems operate, as recently shown for the unprecedented meta−meta′ dimagnesiation of *N*,*N*-dimethylaniline, where the supramolecular structure of the mixed-metal base templates the regioselectivity of the deprotonation process.[4] Extension of some of these studies to transition-metal systems, replacing the low polarity s-block metal by another divalent metal such as Mn(II), Cr(II), or Fe(II), have already hinted at the potential of these systems to display related synergic chemistry.[5] Focusing on Fe(II) ferrate complexes, direct ferration of substituted aromatic substrates has been reported using mixed

Received: July 24, 2015
Published: September 2, 2015

DOI: 10.1021/acs.inorgchem.5b01638
Inorg. Chem. 2015, 54, 9201−9210

lithium−iron bases which contain the bulky amide group TMP (TMP = 2,2,6,6-tetramethylpiperidide).[6,7] Interestingly in some cases the in situ generated functionalized aryl ferrate intermediates can subsequently undergo Ni-catalyzed cross-coupling reactions with organic halides.[6] In closely related work, Mulvey has shown that structurally defined sodium ferrate [(TMEDA)NaFe(TMP)(CH_2SiMe_3)$_2$] (TMEDA = *N,N,N′,N′*-tetramethylethylenediamine) promotes the regioselective 2-fold ferration of benzene at the sterically optimal 1- and 4-positions, affording a unique iron-host inverse-crown complex.[5a] More recently, Bedford has elegantly disclosed the key involvement of homoleptic aryl ferrates in iron-catalyzed Kumada coupling processes.[8] Surprisingly, despite their synthetic relevance and the increasing attention that organoiron chemistry is currently being paid,[9] the number of structurally defined alkali-metal ferrates still remains scarce.[10]

Running in parallel to this research has been that of iron complexes containing N-heterocyclic carbene ligands (NHCs),[11] which have found numerous applications in catalytic transformations, including C−C and C−N bond formation processes.[12] Although in many cases the nature of the active iron species implicated in these transformations has not been made forthcoming, the involvement of low-coordinate Fe NHC complexes has been postulated,[13] which have sparked widespread interest in the synthesis and reactivity of this particular type of compound.[11,14]

Merging these two evolving fields in synthesis together, namely cooperative bimetallics and NHC-Fe chemistry, here we report our findings on the synthesis of a new series of NHC-stabilized sodium ferrates containing the unsaturated carbene **IPr** (**IPr** = 1,3-bis(2,6-di*iso*propylphenyl)imidazol-2-ylidene). Combining X-ray crystallography and spectroscopic studies with SQUID magnetization investigations, we assess the constitution and reactivity of this family of complexes, unveiling a method that grants access to a three-coordinate abnormal-NHC Fe complex.

RESULTS AND DISCUSSION

Synthesis of Donor-Solvent-Free Sodium Ferrates. Building on our previous studies on the synthesis of alkali-metal magnesiate and zincate complexes,[15,16] we started our investigation assessing the cocomplexation reaction between Fe(II) amide Fe(HMDS)$_2$ (HMDS = 1,1,1,3,3,3-hexamethyldisilazide, N($SiMe_3$)$_2$)[17] and the sodium amide NaHMDS or the monosilyl derivative $NaCH_2SiMe_3$[18] in the noncoordinating solvent hexane. Although both sodium compounds are sparingly soluble in hexane, addition of the Fe bis(amide) and gentle heating afforded dark green homogeneous solutions, which deposited green crystals of homoleptic and heteroleptic donor-solvent-free sodium ferrates [{NaFe(HMDS)$_3$}$_\infty$] (**1**) and [{NaFe(HMDS)$_2$(CH_2SiMe_3)}$_\infty$] (**2**) in 80% and 73% yields, respectively (Scheme 1).

As determined by X-ray crystallography, the structures of contact ion pair ferrates **1** and **2** were found to be based on a planar four-membered {NaNFeN} ring (Figures 1a and 2a, respectively), where both metals are connected by two HMDS bridges, while the remaining anionic ligand (HMDS or CH_2SiMe_3 for **1** and **2**, respectively) occupies a third (terminal) coordination site on Fe. Coordinatively unsaturated within these asymmetric units, the solvent-free sodium centers in **1** and **2** attain higher coordination numbers by forming intermolecular interactions with the HMDS groups of adjacent molecular units (via Na···Me electrostatic contacts), which

Scheme 1. Synthesis of Donor-Solvent-Free Sodium Ferrates 1 and 2

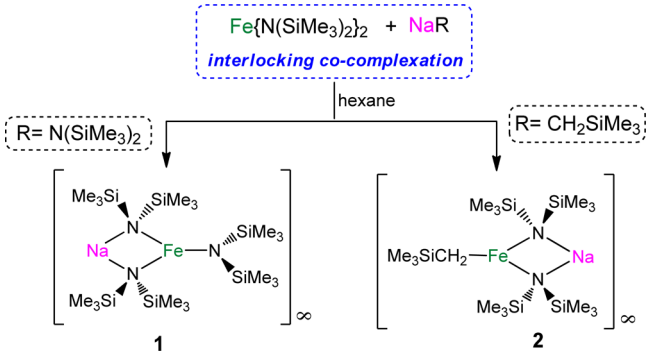

afford in both cases new 1D polymeric chain structures (Figures 1b and 2b, respectively). Thus, for **1** each Na interacts with a single Me group from the terminal HMDS ligand of a neighboring {NaFe(HMDS)$_3$} fragment (Na(1)−C18, 2.838(4) Å), giving rise to a linear head-to-tail arrangement (Figure 1b). This motif is in marked contrast to the discrete monomeric structure recently reported for the lithium analogue of **1**, [LiFe(HMDS)$_3$],[10g] where Li attains a tetrahedral geometry by forming two intramolecular Li···Me(HMDS) contacts.[19] Donor-free alkali-metal ate structures are rare in heterobimetallic chemistry,[20] and as far as we are aware, the structure of **1** and that of the lithium ferrate mentioned above constitute the first examples of homoleptic HMDS-based ates containing a divalent transition metal.[21] Understandably, the mean Fe−N bond length for the bridging HMDS ligands in **1** (2.034 Å) is slightly elongated in comparison to the terminal Fe1−N3 (1.964(2) Å). These values are in good agreement with those reported for the THF adduct [(THF)NaFe(HMDS)$_3$],[22] which also exhibits a contact ion pair structure, with a three-coordinated distorted-trigonal-planar Fe(II) center,[23] and they show very little variation from those found in the solvent-free lithium ferrate mentioned above[10g] or in the neutral iron bis(amide) [{Fe(HMDS)$_2$}$_2$] (mean values of 2.084 and 1.925 Å for bridging and terminal Fe−N distances, respectively).[17b] Interestingly, this THF solvate has been prepared using an synthetic method alternative to that described for **1**, by reducing Fe(III) amide Fe(HMDS)$_3$ with the sodium silanide (THF)$_2$Na(Si*t*Bu$_3$) and coformation of the disilane *t*Bu$_3$Si−Si*t*Bu$_3$.[22] Having a mean value of 2.497 Å, the Na−N distances in **1** show a noticeable variation from those in the dimeric sodium complex [{(*t*BuCN)$_2$Na(HMDS)}$_2$] (2.405 Å),[24] where the Na centers are also tricoordinated, although in this case the NNaN bond angle is significantly more obtuse than in **1** (100.3(1) vs 84.03(9)°).[25] These structural features can be rationalized considering the different nature of the metal−N bonds present in this heterobimetallic species. Thus, the shorter and more covalent anchoring Fe−N bonds provide the foundations for the {Fe(HMDS)$_3$}$^-$ units, to which the sodium cations are affixed by a combination of weaker Na−N and Na···CH_3 ancillary bonds.[26]

In contrast with the linear arrangement of **1**, heteroleptic sodium ferrate **2** exists as a zigzag chain polymer (Figure 2b) comprising {NaFe(HMDS)CH_2SiMe_3} units connected in a head-to-head arrangement via Na···Me(HMDS) medium-long electrostatic interactions (Na(1)−C2 2.854(2), Na1−C12(2) 3.041(2) Å), with the terminal alkyl groups attached to the Fe atoms and running along opposite edges of the chain in a

DOI: 10.1021/acs.inorgchem.5b01638
Inorg. Chem. 2015, 54, 9201−9210

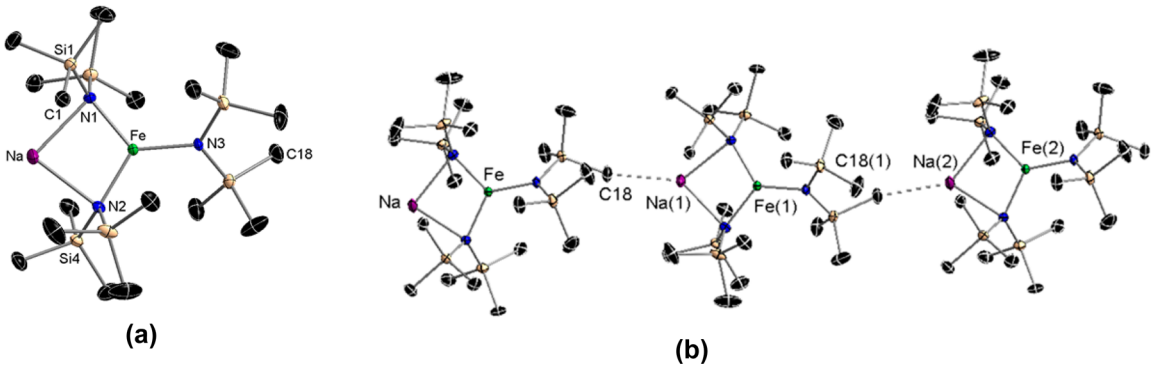

Figure 1. (a) Asymmetric unit of $[\{NaFe(HMDS)_3\}_\infty]$ (**1**). Hydrogen atoms are omitted for clarity. Thermal ellipsoids are displayed at the 50% probability level. Selected bond distances (Å) and angles (deg): Fe−N1 2.036(2), Fe−N2 2.032(2), Fe−N3 1.964(2), Fe···Na 3.0131(13), Na−N1 2.502(3), Na−N2 2.492(3); N1−Fe−N2 110.48(10), N1−Fe−N3 124.93(10), N2−Fe−N3 124.56(10), Na−N1−Fe 82.51(8), Na−N2−Fe 82.86(8), Na−Fe−N3 176.00(9), N1−Na−N2 84.03(9). (b) Section of the polymeric chain showing propagation and selected atom labeling. Na(1)−C18 2.838(4) Å.

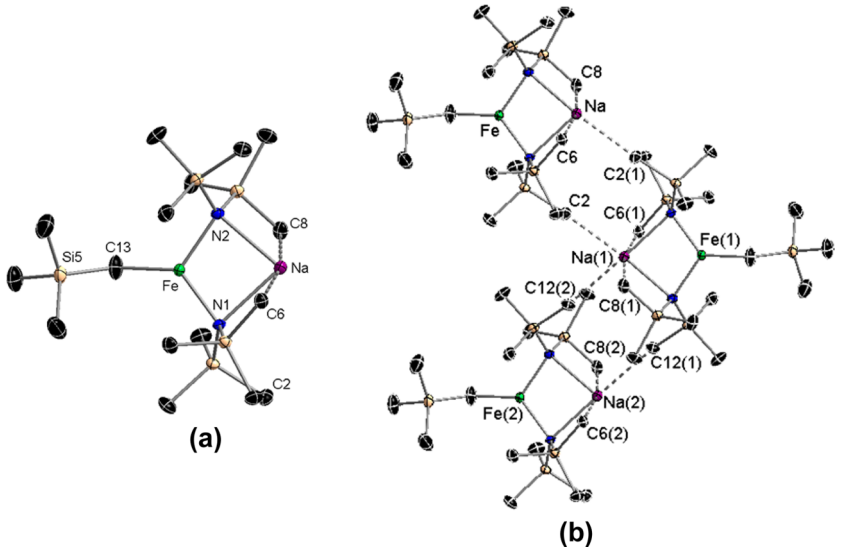

Figure 2. (a) Asymmetric unit of $[\{NaFe(HMDS)_2(CH_2SiMe_3)\}_\infty]$ (**2**). Hydrogen atoms are omitted for clarity. Thermal ellipsoids are displayed at the 50% probability level. Selected bond distances (Å) and angles (deg): Fe−N1 2.0308(17), Fe−N2 2.0306(17), Fe−C13 2.051(2), Na−C6 2.7013(21), Na−C8 2.7275(21), Fe···Na 3.0401(9), Na−N1 2.4804(19), Na−N2 2.4702(19); N1−Fe−N2 107.96(7), N1−Fe−C13 129.08(10), N2−Fe−C13 121.83(10), Na−N1−Fe 84.11(6), Na−N2−Fe 84.38(6), Na−Fe−C13 165.55(7), N1−Na−N2 83.14(6). (b) Section of the polymeric chain showing intermolecular and intramolecular Na−Me contacts. Na1−C2 2.838(4) Å, Na(1)−C12(2) 3.041(2) Å.

staggered fashion. Illustrating the structural similarities of Mn(II) and Fe(II) in heterobimetallic chemistry, this motif is almost identical with that described by Mulvey and Klett for $[NaMn(HMDS)_2CH_2SiMe_3]$.[27,28] The propagation mode in **2**, exclusively involving Na···Me bonds, contrasts with that found in the related magnesiate $[\{NaMg(HMDS)_2Bu\}_\infty]$, which polymerizes via the anionic C of the butyl group, giving rise to a linear chain.[20c] In contrast, in **2** the monosilyl group binds terminally to Fe (Fe−C13 2.051(2) Å).[29] The main geometrical parameters within the dinuclear {NaNFeN} ring show little variation from those discussed for **1**, although in **2** the sodium atom receives additional stabilization within the asymmetry unit by forming two intramolecular Na···Me contacts (Na−C8, 2.7275(21), Na1−C6, 2.7013(21) Å) (Figure 2a), which are noticeably shorter than its propagating intermolecular interactions (vide supra). Thus, while the Fe center in **2** has a distorted-trigonal-planar geometry similar to that of **1** (sum of the internal angles around Fe is 359.97°, ranging from 107.96(10) to 129.08(10)°), the sodium atoms in **2** reach hexacoordination by bonding to two N atoms and four Me(HMDS) groups (while in **1** Na exists in a tricoordinate environment).

Compounds **1** and **2** both exhibit good solubility in C_6D_6, suggesting that their polymeric structures observed in the solid state are not retained in solution. The paramagnetic character of these heterobimetallic compounds is manifested in the broad paramagnetically shifted resonances observed in their ^1H and ^{13}C NMR spectra. Reflecting the ferrate constitution of **1**, its ^1H NMR spectrum shows a broad signal at −4.72 ppm for the $SiMe_3$ groups, which is moved drastically upfield from the corresponding resonance found for the $Fe(HMDS)_2$ precursor in the same deuterated solvent (at 60.27 ppm). The solution-phase magnetic moment of **1** was found to be 4.72 μ_B (determined by the Evans method),[30] which is close to the expected value (4.90 μ_B) for a high-spin ($S = 2$) Fe(II) center.[31] The ^1H NMR spectrum of **2** displayed two distinct $SiMe_3$ resonances easily assignable for the HMDS groups (at −8.57 ppm integrating for 36H) and for the monosilyl ligand (at

DOI: 10.1021/acs.inorgchem.5b01638
Inorg. Chem. 2015, 54, 9201−9210

Scheme 2. Synthesis of NHC-Stabilized Sodium Ferrates (a) 3, (b) 4, and (c) Heteroleptic Ferrate 5 via an Indirect Ferration Approach

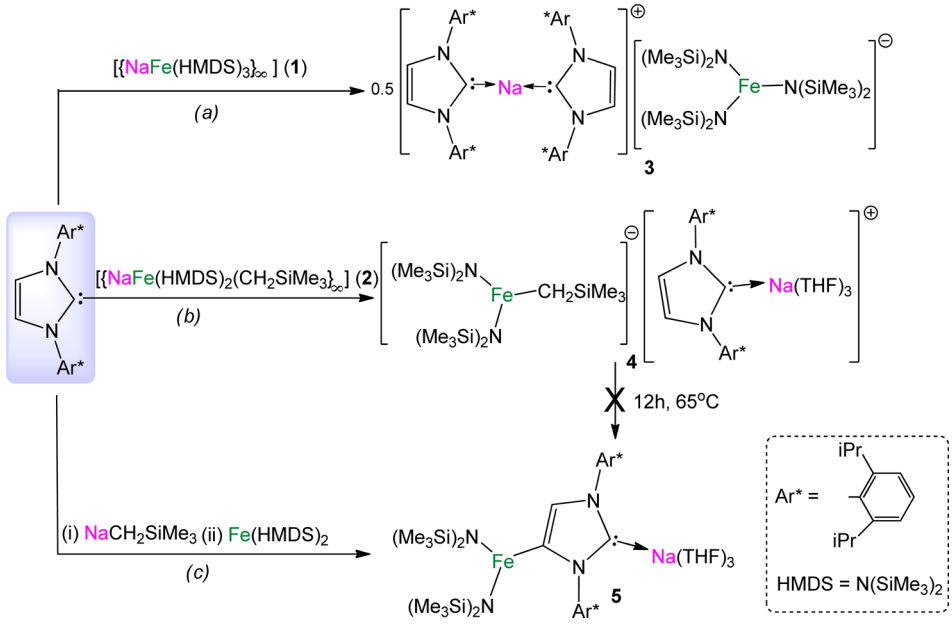

13.51 ppm integrating for 9H) (see the Supporting Information for details).[32,33]

Reactivity Studies using the NHC IPr. Next we investigated the reactivity of sodium ferrates with unsaturated NHC **IPr**, finding that treating hexane solutions of each bimetallic compound with equimolar amounts of this carbene led to a significant color change (from green to light brown) and the formation of insoluble products. Addition of fluorobenzene in the case of **1** and THF for **2** afforded crystals of the NHC-stabilized sodium ferrates $[Na(IPr)_2]^+[Fe(HMDS)_3]^-$ (**3**) and $[(THF)_3{\cdot}NaIPr]^+[Fe(HMDS)_2CH_2SiMe_3]^-$ (**4**), respectively, in 35 and 70% yields (note that the yield of **3** can rise to 73% by employing 2 equiv of **IPr**) (Scheme 2a,b).

X-ray crystallographic studies established the molecular structures of **3** and **4**. In each case the infinite polymeric arrangement of sodium ferrates **1** or **2** has deaggregated to form discrete monomeric solvent-separated ion pair structures where the NHC ligands act as neutral lone-pair donors stabilizing the alkali metal (Figures 3 and 4). The molecular structure of **3** comprises a cationic moiety where the Na center is solvated by two neutral **IPr** ligands in a near-linear disposition (C–Na–C bond angle 168.95(17)°) and an anionic ferrate moiety featuring a strictly planar tricoordinate Fe(II) center (sum of N–Fe–N angles 360°), with a mean Fe–N bond length of 1.993 Å. Consistent with its anionic constitution, this Fe–N bond distance is understandably longer in comparison to that found in the related neutral Fe(III) tris(amide) $Fe(HMDS)_3$ (1.917(4) Å),[34] which also exhibits a trigonal-planar geometry around Fe. It should be noted that the anion moiety of **3** has been previously reported by Dehnicke and co-workers in the structure of $[Na(12\text{-crown-}4)_2]^+[Fe(HMDS)_3]^-$, but made in a different way by reduction of the Fe(III) precursor $Fe(HMDS)_3$ with NaHMDS in the presence of the metal sequestering ligand 12-crown-4 ether.[35] Interestingly, the structure of **3** bears a strong resemblance to the sodium magnesiate $[Na(IPr)_2]^+[Mg(HMDS)_3]^-$ reported by Hill,[36] which contains the same cationic moiety, with the Na and Mg

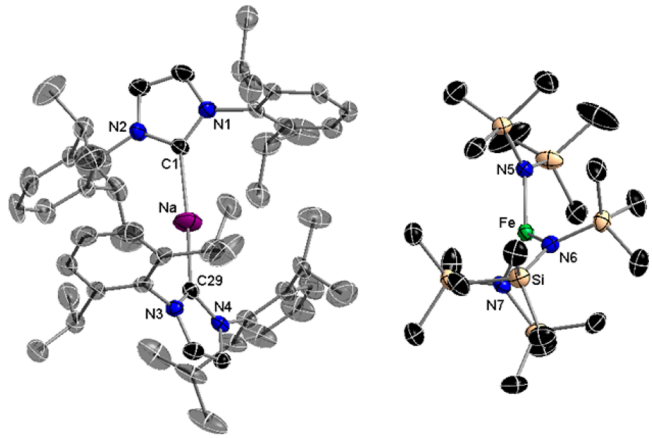

Figure 3. Molecular moieties of the X-ray crystal structure of compound $[Na(IPr)_2]^+[Fe(HMDS)_3]^-$ (**3**) with selective atom labeling. Hydrogen atoms and disorder components in isopropyl groups are omitted for clarity. Thermal ellipsoids are displayed at the 50% probability level. Selected bond distances (Å) and angles (deg): Fe–N5 1.996(3), Fe–N6 1.993(3), Fe–N7 1.990(3), Na–C1 2.445(4), Na–C29 2.460(4), C1–N1 1.360(5), C1–N2 1.362(5), C29–N3 1.363(5), C29–N4 1.362(5); N5–Fe–N6 121.15(13), N5–Fe–N7 119.66(13), N6–Fe–N7 119.20(13), C1–Na–C29 168.95(17), Na–C1–N1 137.4(3), Na–C1–N2 120.2(3), N1–C1–N2 102.3(3), Na–C29–N3 142.9(3), Na–C29–N4 114.7(3), N3–C29–N4 102.3(3).

centers exhibiting an coordination environment almost identical with those described above for Na and Fe, respectively, in **3**.

Diverging from **3**, the Na center in **4** binds to only one **IPr** ligand but completes a distorted-tetrahedral geometry by coordinating three molecules of the donor solvent THF (average angle around Na, 108.7°, values ranging from 89.5(6) to 126.5(6)°). Although the structure of this cation is not known, the coordination around Na is almost identical with that described in the sodium zincate $[(THF)_3Na[:C\{[N(2,6\text{-}iPr_2C_6H_3)]_2CHCZn(t\text{Bu})_2\}]$, which contains an anionic

DOI: 10.1021/acs.inorgchem.5b01638
Inorg. Chem. 2015, 54, 9201–9210

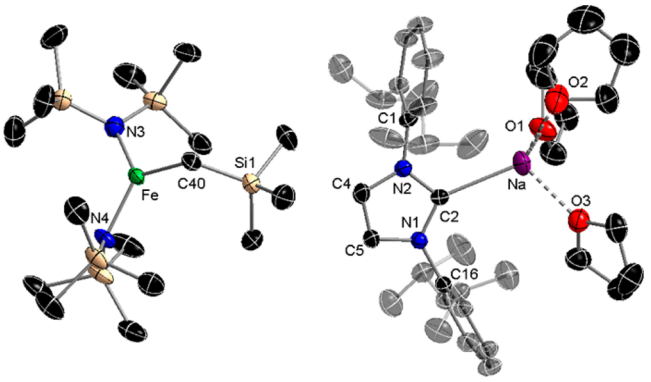

Figure 4. Molecular structure of $[(THF)_3{\cdot}NaIPr]^+[Fe(HMDS)_2CH_2SiMe_3]^-$ (**4**). Hydrogen atoms and disorder components in isopropyl, THF, and $SiMe_3$ groups are omitted for clarity. Thermal ellipsoids are displayed at the 50% probability level. Selected bond distances (Å) and angles (deg): Fe–N3 1.982(2), Fe–N4 1.989(2), Fe–C40 2.065(3), C40–Si1 1.831(3), Na–C2 2.551(3), Na–O1 2.348(2), Na–O2 2.32(3), Na–O3 2.307(2), C2–N1 1.365(3), C2–N2 1.363(3); N3–Fe–N4 123.40(10), N3–Fe–C40 119.56(11), N4–Fe–C40 116.84(11), Na–C2–N1 121.30(16), Na–C2–N2 121.30(16), N1–C2–N2 101.9(2), C2–Na–O1 122.69(9), C2–Na–O2 126.5(6), C2–Na–O3 110.69(9), O1–Na–O2 89.5(6), O1–Na–O3 101.60(9), O2–Na–O3 101.3(5).

version of the NHC ligand IPr[37] that coordinates to a $\{Na(THF)_3\}$ cation via its C2 position, forming a Na–C bond of 2.501(3) Å of strength similar to that found in **4** (Na–C2 2.551(3) Å). The structure of **4** is completed by the new heteroleptic ferrate anion $\{Fe(HMDS)_2CH_2SiMe_3\}^-$, which as a consequence of its lack of interaction with the Na cente exhibits a significantly wider NFeN bond angle (123.40(10)°) and slightly shorter Fe–N bond distances (1.985 Å) in comparison to those observed in the contact ion pair precursor **2** (107.96(7)° and 2.031 Å).

The ^{1}H NMR spectra of **3** and **4** in d_8-THF (see the Supporting Information) show well resolved sets of resonances assignable to the **IPr** ligands, appearing at almost the same chemical shifts as those found for the free carbene, suggesting that in this ethereal solvent the sodium center is solvated by d_8-THF molecules rather than by the neutral sterically imposing NHC. In addition, for **3**, a broad low-frequency resonance is observed at −2.39 ppm, which can be assigned to the HMDS groups bound to the paramagnetic Fe(II) center. In the case of **4** the $SiMe_3$ resonances appear at −3.77 and 7.80 ppm for the HMDS and monosilyl groups, respectively. The solution-phase magnetic moments of **3** and **4** (4.90 and 4.40 μ_B, respectively) determined using the Evans method are consistent with a high-spin $S = 2$ configuration.

The formation of coordination products **3** and **4** in the reactions of sodium ferrates **1** and **2** with **IPr** is in contrast with our previous findings using a related family of amido-based bimetallic reagents, in particular sodium zincates, which can promote the deprotonation of several unsaturated NHCs at the "abnormal" C4 position of the imidazole ring under mild reaction conditions via a direct zincation process.[37] Even under harsher reaction conditions, by heating the reaction mixtures at 70 °C for 12 h, only adducts **3** and **4** were obtained. We next attempted the synthesis of a ferrate complex containing an anionic NHC[38] using an indirect approach, by treating the three-coordinate NHC complex $[(IPr)Fe(HMDS)_2]$[39] with either of the sodium reagents NaHMDS and $NaCH_2SiMe_3$. Interestingly these reactions also yielded complexes **3** and **4**, respectively, revealing that under these conditions the polar sodium reagents not only fail to metalate **IPr** but also maintain the preference of the iron(II) bis(amido) fragment to coordinate to another anionic ligand (either HMDS or CH_2SiMe_3) rather than to the neutral NHC. Interestingly, similar reactivity has been noted by us for alkylzinc and alkylgallium NHC complexes, which when treated with organolithium reagents form the relevant cocomplexation lithium ate species, with the NHC ligand coordinated to Li.[37,40] On the other hand, in contrast with these studies, Robinson has demonstrated that when the free **IPr** is treated with BuLi the straightforward selective lithiation of the NHC occurs at the C4 position of the imidazole ring, affording a novel anionic carbene lithium complex.[41] Inspired by this pioneering metalating work, we first treated **IPr** in hexane with an equimolar amount of the sodium alkyl $NaCH_2SiMe_3$, leading almost instantaneously to a white solid which was subsequently reacted with 1 equiv of $Fe(HMDS)_2$. Introduction of THF afforded a green-brown solution which upon cooling to −30 °C deposited green crystals of heteroleptic ferrate $(THF)_3Na[:C\{[N(2,6\text{-}^iPr_2C_6H_3)]_2CHCFe(HMDS)_2\}]$ (**5**) in 60% yield (Scheme 2c).

X-ray crystallographic studies established the contacted ion pair structure of **5** (Figure 5), where the carbene has now been

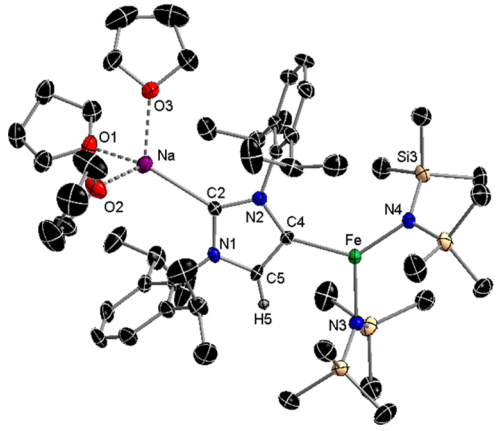

Figure 5. Molecular structure of complex **5** with selective atom labeling. Hydrogen atoms are omitted for clarity. Thermal ellipsoids are displayed at the 50% probability level. Selected bond distances (Å) and angles (deg): Fe–C4 2.085(4), Fe–N3 1.998(3), Fe–N4 1.973(3), Na–C2 2.510(4), Na–O1 2.336(3), Na–O2 2.313(3), Na–O3 2.286(3), C2–N1 1.357(4), C2–N2 1.371(4); C4–Fe–N3 105.15(14), C4–Fe–N4 131.45(14), N3–Fe–N4 123.39(13), Fe–C4–N2 139.3(3), Na–C2–N1 121.3(2), Na–C2–N2 136.9(3), N1–C2–N2 101.7(3).

incorporated into the ferrate scaffold acting as an anionic ligand, coordinating through its *normal* C2 position to Na (Na–C2 2.510(4) Å), while Fe occupies the position previously filled by an H atom, bonding to the C4 position (Fe–C4 2.085(4) Å). Understandably this distance is shorter than that reported for the *abnormal* complex $[(aIPr)Fe(HMDS)_2]$,[42] which also displays a tricoordinate Fe atom connected to two HMDS groups and to the C4 position of a neutral NHC ligand. In agreement with its anionic ate constitution, its Fe–N distances (Fe–N3 1.998(3) Å; Fe–N4 1.973(3) Å) are similar to those found for the homoleptic anion of **3** (average Fe–N 1.993 Å) and are slightly elongated from

DOI: 10.1021/acs.inorgchem.5b01638
Inorg. Chem. 2015, 54, 9201–9210

those reported for [(*a*IPr)Fe(HMDS)$_2$][42] (average Fe−N 1.962 Å). On comparison of the molecular structures of **4** and **5**, it could be tempting to describe **4** as a premetalation complex of **5**; however, it should be noted that **4** is a stable species that does not evolve to **5** even under forcing reaction conditions (70 °C, 12 h), which makes this assumption very unlikely. This highlights the importance of the synthetic methods employed and the remarkable differences that can be realized in bimetallic chemistry by having the two metals operate in either a stepwise or synchronous manner.[1]

The ^{1}H NMR spectrum of **5** in C_6D_6 exhibits a series of broad resonances in the range +10.59 to −6.94 ppm, including a signal at −4.21 ppm, which integrating for 36 H can be assigned to the HMDS hydrogen atoms. In addition, another broad low-frequency resonance is observed at −26.37 ppm, which has been attributed to the C*H* fragment of the imidazolyl ring (see the Supporting Information). The complexity and broadness of this NMR spectrum are in contrast with the relative simplicity and good resolution of the spectra recorded for **3** and **4**, where neutral **IPr** is not attached to a paramagnetic Fe(II) center.

The formation of **5** can be rationalized in terms of a stepwise indirect ferration process. Initially **IPr** is deprotonated at its C4 position by the polar organosodium reagent to form Na$^+$IPr$^-$, which in turn undergoes transmetalation with the more electronegative iron bis(amide). Although the white powder obtained by reacting **IPr** with $NaCH_2SiMe_3$ cannot be characterized spectroscopically due to its complete lack of solubility in organic solvents such as THF and toluene, the isolation of **5** provides compelling proof that the metalation of the NHC has occurred.[43]

C4 deprotonation of unsaturated NHCs constitutes one of the main synthetic routes to access anionic (or ditopic) NHCs.[38,44] To date, only two efficient metalating reagents have proved capable of selectively abstracting an H from the imidazole ring of **IPr**: monometallic ^{n}BuLi[41,45] and the mixed-metal system [(TMEDA)NaZn(TMP)^{t}Bu$_2$].[37,46] Our studies show that sodium alkyl $NaCH_2SiMe_3$ can also promote the selective metalation (Na−H exchange) reaction of the imidazole ring at its C4 position. Related to the synthesis of **5**, it should be noted that Goicoechea has recently demonstrated the reduction of [Fe(IPr)(Mes)$_2$] (Mes = mesityl) with potassium graphite which allows for the isolation of the iron complex K[{:C[N(2,6-^{i}Pr$_2$C$_6$H$_3$)]$_2$(CH)C}$_2$Fe(Mes)] containing two anionic carbenes, both bound through their C4 position to Fe.[47] This compound is formed in a 26% yield as a result of a redistribution process, with the concomitant formation of a tris(mesityl) potassium ferrate and H_2.

Abnormal NHC-Fe Complex via Electrophilic Interception. Recent studies in main-group chemistry have shown that certain anionic NHC complexes when treated with a suitable electrophile such as HCl·NEt$_3$ or MeOTf can be transformed into their neutral abnormal adducts, where the imidazole ring of the NHC binds to the metal through its backbone (using its C4 position).[48] Although within transition metals abnormal carbene complexes are more abundant than those with s- and p-block elements,[49] the number of Fe complexes containing these ligands is still limited to just a few recent examples.[50] Some of these studies employ pincer ligands,[50a] whereas Grubbs has used Bertrand's isolable *abnormal* carbene (*a*NHC = 1,3-bis(2,6-diisopropylphenyl)-2,5-diphenyl-imidazol-4-ylidene)[51] to trap and stabilize an unique intermediate diiron cyclooctatetraenyl (COT) complex.[50b] More recently, Layfield has reported a thermally induced rearrangement of [(IPr)Fe(HMDS)$_2$], which after 3 h in refluxing toluene solution evolves to its abnormal isomer [(*a*IPr)Fe(HMDS)$_2$].[42] Intrigued by these precedents, we next pondered whether electrophilic interception of anionic NHC complex **5** could also allow access to neutral abnormal Fe complexes. Thus, **5** was treated with 1 molar equiv of MeOTf at −78 °C in toluene (Scheme 3). The reaction took place with

Scheme 3. Electrophilic Interception of Anionic NHC Complex 5 with MeOTf

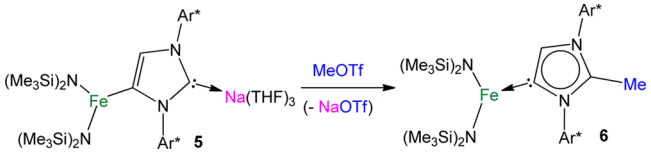

the formation of a white precipitate (presumably NaOTf), affording the neutral abnormal Fe NHC complex [CH$_3$C{[N-(2,6-*i*Pr$_2$C$_6$H$_3$)]$_2$CHCFe(HMDS)$_2$}] (**6**) as a yellow crystalline solid in 28% isolated yield. Compound **6** is obtained as the result of the selective methylation of the C2 position of the anionic NHC ligand present in **5**, leaving its Fe−C4 bond and more importantly the Fe−N bonds intact. This is particularly noteworthy, as recent studies have shown that the amido groups in the related complex [IPr.Fe(HMDS)$_2$] can display basic lability, metalating substrates such as PhSeH with the subsequent formation of HMDS(H).[31c]

The molecular structure of **6** was established by X-ray crystallographic studies (Figure 6). The bond length of

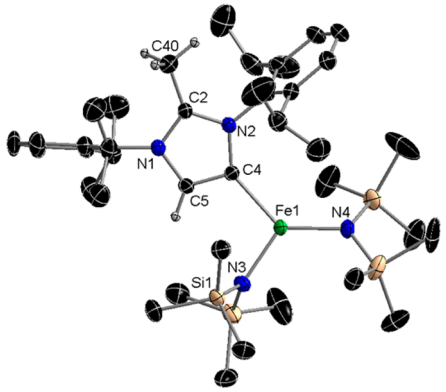

Figure 6. Molecular structure of complex **6** with selective atom labeling. Hydrogen atoms and minor disorder components in SiMe$_3$ groups are omitted for clarity. Thermal ellipsoids are displayed at the 50% probability level. Selected bond distances (Å) and angles (deg): Fe−C4 2.113(2), Fe−N3 1.9732(19), Fe−N4 1.9459(19), C2−N1 1.330(4), C2−N2 1.341(3), C2−C40 1.491(3); C4−Fe−N3 104.02(8), C4−Fe−N4 132.84(8), N3−Fe−N4 123.14(8), Fe−C4−N2 140.30(16), C40−C2−N1 125.3(2), C40−C2−N2 126.9(2), N1−C2−N2 107.46(19).

1.491(3) Å for C2−C40 is consistent with a single bond, while the Fe−C4 bond length (2.113(2) Å) is only slightly elongated with respect to that in the anionic complex **5** (2.085(4) Å) and is almost identical with that reported for [(*a*IPr)Fe(HMDS)$_2$] (2.117(2) Å).[42] Supporting previous studies that have described abnormal NHC ligands as stronger σ-donors than their normal isomers,[51] the Fe−C4 distance in **6**

DOI: 10.1021/acs.inorgchem.5b01638
Inorg. Chem. 2015, 54, 9201−9210

is shorter than that in the related complex containing a normal NHC ligand [(IPr)Fe(HMDS)$_2$] (2.182(2) Å), which also features a tricoordinate Fe center.[39]

The ^{1}H NMR spectrum of paramagnetic **6** in d_8-toluene features a series of broad resonances in the range of +29.37 to −33.29 ppm (Supporting Information). A distinctive, very broad resonance for the C5 hydrogen atom on the imidazole ring can be seen at −33.29 ppm, which is just slightly upfield from that observed for the same proton in ferrate **5** (at −26.37 ppm), while the resonances for the CH_3 group attached to the C2 atom of the carbene and for these of the HMDS groups appear downfield at 29.36 and −5.05 ppm, respectively. Resonances for the aromatic protons are observed at 10.78, 9.64, and 8.58 ppm, while the lack of symmetry in the imidazole ring is evidenced by the presence of two distinct sets of signals for the isopropyl substituents (δ 1.32 and 1.21 ppm for CHs and δ 4.53, 0.98, −3.40, and −6.96 for Me groups).

Magnetic Studies. The electronic structure of the Fe(II) centers in **1**−**6** was studied through bulk magnetization measurements. Thus, molar paramagnetic susceptibility (χ_M) data were collected on microcrystalline samples in the 2−300 K temperature range, under a constant magnetic field of 0.5 T (0.1 T in the case of **3**), in the warming mode. The results are represented in Figure 7 in form of $\chi_M T$ vs T curves. In all cases,

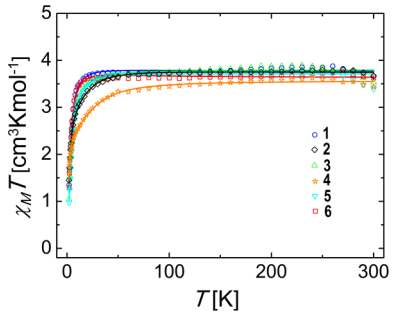

Figure 7. $\chi_M T$ vs T curves of compounds **1**−**6** (measurement setup 2 → 300 K). Solid lines represent the results of the fits.

the $\chi_M T$ product at 300 K is slightly higher than the expected value (3.00 cm^3 K mol^{-1} for g = 2.0) for one uncoupled high-spin (S = 2) iron(II) center (3.67, 3.53, 3.62, 3.39, 3.67, and 3.44 cm^3 K mol^{-1} for **1**−**6**, respectively), indicating that the ligand field is insufficient to force a violation of Hund's rule. The estimated g values using the Curie Law for the room-temperature data are g = 2.21, 2.17, 2.20, 2.13, 2.21, and 2.14, respectively, which suggests the presence of unquenched angular momentum, which in turn is coupled to the electronic spin, thus leading to susceptibility values larger than those calculated for "spin-only" systems. Inspection of the curves reveals that, when the temperature is lowered from 300 K, a slight increase of $\chi_M T$ takes place for all of the compounds, which is attributed to a slight decomposition of the sample occurring upon warming (certainly involving the oxidation to Fe(III)). On analysis of the $\chi_M T$ product below the almost imperceptible maximum (near 260 K), a very slightly positive slope is barely appreciable, most likely explained by the influence of a weak temperature-independent contribution to paramagnetism. Sharp decreases are observed for all the products at the lowest temperatures, leading to $\chi_M T$ values of 1.35, 1.04, 1.30, 0.97, 1.45, and 1.59 cm^3 K mol^{-1} (for **1**−**6**, respectively) at 2 K. This very apparent decline is explained by the effect of zero-field splitting (ZFS), which is another consequence of the presence of spin−orbit coupling. The latter is explained by the nature of the electronic states of Fe(II) in this coordination environment, which in their ground state are expected to lack any orbital angular momentum (L = 0), which is however altered by mixing of electronic excited states with nonzero L. The effects of this mixing can be modeled using perturbation theory. Thus, the experimental data were fit using the program PHI[52] by matrix diagonalization of the (perturbative) anisotropic spin Hamiltonian defined in eq 1:

$$\hat{H} = D\left(\hat{S}_z^{\,2} - \frac{1}{3}\hat{S}^2\right) + E(\hat{S}_x^{\,2} - \hat{S}_y^{\,2}) + \mu_B \cdot (\hat{S}_x g_x B_x + \hat{S}_y g_y B_y + \hat{S}_z g_z B_z) \quad (1)$$

In eq 1, D and E stand for axial and rhombic ZFS parameters, respectively, $\hat{S}$ is the total spin operator, and $\hat{S}_i$ (i = x, y, z) are the operators of its components. B_i (i = x, y, z) are the components of the magnetic induction, and μ_B is the Bohr magneton. The anisotropy of the g factor was considered by setting $g_x = g_y \neq g_z$, which takes into account the trigonal-planar coordination environment around Fe(II). No intermolecular interactions were considered, given the large distance between paramagnetic centers.

The results from the fitting are collected in Table 1. For compounds **1** and **3**, the best fits reveal the presence of axial zero-field splitting (D values of +7.5 and +8.3 cm^{-1}, respectively, and E = 0) with anisotropic g values, where $g_x = g_y > g_z$. These parameters are in accordance with the consistency criterion derived from perturbation theory defined as $D = 0.5\,\lambda(g_z - g_x)$,[53] taking a value of the spin−orbit coupling parameter λ for Fe(II) close to the that of the free ion (−102 cm^{-1}).[54] Quite similar values were previously reported for the related compound [Li(15-crown-5)]$^+$[Fe{N(SiMe$_3$)$_2$}$_3$]$^-$, which exhibits a higher degree of axiality.[31d] Heteroleptic compounds **2** and **4** follow a pattern of behavior almost identical with that of the above systems (D values of +9.6 and +10.2 cm^{-1}, respectively, and E = 0). These values of D suggest that replacing one [N(SiMe$_3$)$_2$]$^-$ ligand with [CH$_2$SiMe$_3$]$^-$ does not modify significantly the crystal field

Table 1. Fitting Parameters for Compounds 1−6

complex	$\chi_M T$[a] at room temp (g)	μ_{eff}[b] at room temp	$\chi_M T$[a] at 2 K	$g_x = g_y$	g_z	D (cm^{-1})	E (cm^{-1})
1	3.67 (2.21)	5.42	1.35	2.30	2.12	7.5	0.0
2	3.53 (2.17)	5.32	1.04	2.23	2.28	9.6	0.0
3	3.62 (2.20)	5.38	1.30	2.30	1.97	8.3	0.0
4	3.39 (2.13)	5.21	0.97	2.26	2.15	10.2	±0.1
5	3.67 (2.21)	5.42	1.45	2.17	2.35	−15.5	±4.2
6	3.44 (2.14)	5.25	1.59	2.21	2.12	−17.7	±0.7

[a]In units of cm^3 K mol^{-1}. [b]In units of Bohr magnetons.

DOI: 10.1021/acs.inorgchem.5b01638
Inorg. Chem. 2015, 54, 9201−9210

around the Fe(II) ion, as can be expected, bearing in mind the structural and electronic similarity of those ligands. The slightly differing effect on the magnetic properties can however be interpreted in terms of the different donor characters of the ligands (see below).

In contrast to this, the fits for compounds **5** and **6** led to negative D values (−15.5 and −17.7 cm^{-1}, respectively) with the appearance of a rhombic zero-field splitting parameter, E (±4.2 and ±0.7 cm^{-1}). The latter is the natural consequence of the deviation from the idealized trigonal environment around the metal ion resulting from the presence of NHC ligands, which introduce a new interaction with the metal d orbitals due to the π donating character of the heterocycles. In fact, this not only generates rhombicity but also changes the sign of the anisotropy, turning axial instead of an easy plane. A drastic change in anisotropy of 3d metals as a result of changes to the π donor properties of ligands, as observed here, has been previously predicted theoretically.[56] The anisotropy to the g factor (Table 1) is featured in these fits by components not differing significantly but leading to two qualitative distinct behaviors; for **6**, $g_x = g_y > g_z$, while for **5**, $g_z > g_x = g_y$. This means that **6** does not comply with the aforementioned criterion, which could be explained by the presence of strong spin−orbit coupling interactions. The latter weakens the accuracy of the perturbative model assumed with the spin Hamiltonian of eq 1. In any case, the observations are perfectly in line with the behavior revealed by other complexes of the $[Fe(HMDS)_2L]$ type (where L = neutral ligand such as PCy_3, THF, or IPr) previously reported, all exhibiting negative D parameters and moderate E values that can be fine-tuned by changing the substituents on the ligands employed (see Table S2 in the Supporting Information for details).[10g,31d,39,55] On the other hand, the important effect on the anisotropy caused by the π bonding character of the NHC donors present in **5** and **6** is very significant, and to the best of our knowledge, it is revealed here for the first time. The gradation of D is also reflected in the values of $\chi_M T$ at low temperatures, which follow the order $\{Fe(HMDS)_2CH_2SiMe_3\}^- \approx [\{NaFe(HMDS)_2(CH_2SiMe_3)\}_\infty] < \{Fe(HMDS)_3\}^- \approx [\{NaFe(HMDS)_3\}_\infty] < (THF)_3Na[:C\{[N(2,6\text{-}iPr_2C_6H_3)]_2CHCFe(HMDS)_2\}] < [CH_3C\{[N(2,6\text{-}iPr_2C_6H_3)]_2CHCFe(HMDS)_2\}]$. The negative D parameter values for **5** and **6** are consistent with this (which imply population of states with higher angular momenta at lower temperatures). For the other complexes, this is a consequence of the stronger σ-donor character of the carbanion over the amido ligand, which for a positive D parameter implies a larger population of the diamagnetic ground state at lower temperatures.

CONCLUSIONS

The new solvent-free sodium ferrates **1** and **2** have been synthesized straightforwardly by cocomplexation of $Fe(HMDS)_2$ with the sodium reagents NaHMDS and $NaCH_2SiMe_3$, respectively. The complicated polymeric arrangements of **1** and **2** can be broken down by introducing the unsaturated carbene **IPr** to form the discrete NHC separated ion pair ferrate **3** and partially NHC separated (THF is also needed) ion pair **4**, respectively. In these complexes the **IPr** neutral donor coordinates preferentially to the Na atom, while the more Lewis acidic Fe is coordinated exclusively to anionic ligand sets. Interestingly, **3** and **4** were also obtained when the NHC complex $[(IPr)Fe(HMDS)_2]$ was treated with NaHMDS and $NaCH_2SiMe_3$, respectively. Contrastingly, sequentially reacting **IPr** with $NaCH_2SiMe_3$ and then $Fe(HMDS)_2$ allows the isolation of heteroleptic ferrate **5**, where both metals are connected by an anionic NHC. Compound **5** can be envisaged as a product of an indirect ferration process, where **IPr** is first metalated (sodiated) by the polar sodium reagent, which in turn undergoes fast transmetalation with $Fe(HMDS)_2$. Collectively these findings illustrate the significantly different outcomes that are possible in mixed-metal chemistry, when the synergy created by two metals operates simultaneously in one molecule or in a stepwise manner in two molecules. In a new approach in transition-metal chemistry, treatment of **5** with equimolar amounts of MeOTf led to the isolation of the tricoordinate neutral iron abnormal NHC complex **6** together with NaOTf. Studies probing the magnetic susceptibility properties of **1**−**6** have revealed an important change to their anisotropy by replacing a pure σ donor from an idealized trigonal coordination environment (**1**−**4**) by an NHC that can offer π donating character (**5** and **6**).

EXPERIMENTAL SECTION

Full experimental details and characterization data of compounds **1**−**6** are included in the Supporting Information.

ASSOCIATED CONTENT

Supporting Information

The Supporting Information is available free of charge on the ACS Publications website at DOI: 10.1021/acs.inorgchem.5b01638.

Full experimental details and characterization data of compounds **1**−**6** (PDF)

Crystallographic results (CIF)

AUTHOR INFORMATION

Corresponding Author

*E-mail for E.H.: eva.hevia@strath.ac.uk.

Notes

The authors declare no competing financial interest.

ACKNOWLEDGMENTS

We thank the EPSRC and European Research Council (ERC) for their generous sponsorship of this research. GA thanks Spanish MINECO (CTQ2012-32247) and IB thanks the Generalitat de Catalunya for a PhD grant (FI-DGR 2014).

REFERENCES

(1) (a) Mulvey, R. E.; Robertson, S. D. *Top. Organomet. Chem.* **2013**, *47*, 129−158. (b) Uchiyama, M.; Wang, C. *Top. Organomet. Chem.* **2014**, *47*, 159−202.

(2) For recent authoritative reviews in the area see: (a) Mulvey, R. E. *Dalton Trans.* **2013**, *42*, 6676−6693. (b) Mongin, F.; Marchand, A. M. *Chem. Rev.* **2013**, *113*, 7563−7727. (c) Tilly, D.; Chevallier, F.; Mongin, F.; Gross, P. C. *Chem. Rev.* **2014**, *114*, 1207−1257. (d) Klatt, T.; Markiewicz, J. T.; Sämann, C.; Knochel, P. *J. Org. Chem.* **2014**, *79*, 4253−4269.

(3) For selected references see: (a) Blair, V. L.; Kennedy, A. R.; Mulvey, R. E.; O'Hara, C. T. *Chem. - Eur. J.* **2010**, *16*, 8600−8604. (b) Baillie, S. E.; Blair, V. L.; Blakemore, D. C.; Hay, D.; Kennedy, A. R.; Pryde, D. C.; Hevia, E. *Chem. Commun.* **2012**, *48*, 1985−1987. (c) Martínez-Martínez, A. J.; Armstrong, D. R.; Conway, B.; Fleming, B. J.; Klett, J.; Kennedy, A. R.; Mulvey, R. E.; Robertson, S. D.; O'Hara, C. T. *Chem. Sci.* **2014**, *5*, 771−781. (d) Armstrong, D. R.; Garden, J. A.; Kennedy, A. R.; Leenhouts, S. M.; Mulvey, R. E.; O'Keefe, P.; O'Hara, C. T.; Steven, A. *Chem. - Eur. J.* **2013**, *19*, 13492−13503.

DOI: 10.1021/acs.inorgchem.5b01638
Inorg. Chem. 2015, 54, 9201−9210

(e) Baillie, S. E.; Bluemke, T. D.; Clegg, W.; Kennedy, A. R.; Klett, J.; Russo, L.; de Tullio, M.; Hevia, E. *Chem. Commun.* **2014**, *50*, 12859−12862. (f) Clegg, W.; Crosbie, E.; Dale-Black, S. H.; Hevia, E.; Honeyman, G. W.; Kennedy, A. R.; Mulvey, R. E.; Ramsay, D. L.; Robertson, S. D. *Organometallics* **2015**, *34*, 2580−2589.

(4) Martínez-Martínez, A. J.; Kennedy, A. R.; Mulvey, R. E.; O'Hara, C. T. *Science* **2014**, *346* (6211), 834−837.

(5) (a) Alborés, P.; Carrella, L. M.; Clegg, W.; García-Alvarez, P.; Kennedy, A. R.; Klett, J.; Mulvey, R. E.; Rentschler, E.; Russo, L. *Angew. Chem., Int. Ed.* **2009**, *48*, 3317−3321. (b) Blair, V. L.; Carrella, L. M.; Clegg, W.; Conway, B.; Harrington, R. W.; Hogg, L. M.; Klett, J.; Mulvey, R. E.; Rentschler, E.; Russo, L. *Angew. Chem., Int. Ed.* **2008**, *47*, 6208−6211. (c) Blair, V. L.; Carrella, L. M.; Clegg, W.; Klett, J.; Mulvey, R. E.; Rentschler, E.; Russo, L. *Chem. - Eur. J.* **2009**, *15*, 856−863.

(6) Wunderlich, S. H.; Knochel, P. *Angew. Chem., Int. Ed.* **2009**, *48*, 9717−9720.

(7) Nagaradja, E.; Chevallier, F.; Roisnel, T.; Jouikov, V.; Mongin, F. *Tetrahedron* **2012**, *68*, 3063−3073.

(8) Bedford, R. B.; Brenner, P. B.; Carter, E.; Cogswell, P. M.; Haddow, M. F.; Harvey, J. N.; Murphy, D. M.; Nunn, J.; Woodall, C. H. *Angew. Chem., Int. Ed.* **2014**, *53*, 1804−1808.

(9) (a) Sherry, B. D.; Fürstner, A. *Acc. Chem. Res.* **2008**, *41*, 1500−1511. (b) Bedford, R. B. *Acc. Chem. Res.* **2015**, *48*, 1485−1493. (c) *Iron Catalysis in Organic Chemistry*; Plietker, B., Ed.; Wiley-VCH: Weinheim, Germany, 2008. (d) Bedford, R. B.; Brenner, P. B. *Top. Organomet. Chem.* **2015**, *50*, 19−46.

(10) See for example: (a) Scott, J.; Gambarotta, S.; Korobkov, I.; Budzelaar, P. H. M. *J. Am. Chem. Soc.* **2005**, *127*, 13019−13029. (b) Scott, J.; Gambarotta, S.; Korobkov, I.; Budzelaar, P. H. M. *Organometallics* **2005**, *24*, 6298−6300. (c) Fürstner, A.; Martin, R.; Krause, H.; Seidel, G.; Goddard, R.; Lehmann, C. W. *J. Am. Chem. Soc.* **2008**, *130*, 8773−8787. (d) Serrano, C. B.; Less, R. J.; McPartlin, M.; Naseri, V.; Wright, D. S. *Organometallics* **2010**, *29*, 5754−5756. (e) Fürstner, A.; Krause, H.; Lehmann, C. W. *Angew. Chem., Int. Ed.* **2006**, *45*, 440−444. (f) Werncke, C. G.; Bunting, P. C.; Duhayon, C.; Long, J. R.; Bontemps, S.; Sabo-Etienne, S. *Angew. Chem., Int. Ed.* **2015**, *54*, 245−248. (g) König, S. N.; Schneider, D.; Maichle-Mössmer, C.; Day, B. M.; Layfield, R. A.; Anwander, R. *Eur. J. Inorg. Chem.* **2014**, *2014*, 4302−4309.

(11) (a) Ingleson, M. J.; Layfield, R. A. *Chem. Commun.* **2012**, *48*, 3579−3589. (b) Bézier, D.; Sortais, J. B.; Darcel, C. *Adv. Synth. Catal.* **2013**, *355*, 19−33. (c) Riener, K.; Haslinger, S.; Raba, A.; Högerl, M. P.; Cokoja, M.; Hermann, W. A.; Kühn, F. *Chem. Rev.* **2014**, *114*, 5215−5272.

(12) Selected references: (a) Bedford, R. B.; Betham, M.; Bruce, D. W.; Danopoulos, A. A.; Frost, R. M.; Hird, M. *J. Org. Chem.* **2006**, *71*, 1104−1110. (b) Ghorai, S. K.; Jin, M.; Hatakeyama, T.; Nakamura, M. *Org. Lett.* **2012**, *14*, 1066−1069. (c) Agrawal, T.; Cook, S. P. *Org. Lett.* **2013**, *15*, 96−99. (d) Cramer, S. A.; Jenkins, D. M. *J. Am. Chem. Soc.* **2011**, *133*, 19342−19345. (e) Dieskau, A. P.; Holzwarth, M. S.; Plietker, B. *Chem. - Eur. J.* **2012**, *18*, 2423−2429.

(13) Ohki, Y.; Hatanaka, T.; Tatsumi, K. *J. Am. Chem. Soc.* **2008**, *130*, 17174−17186.

(14) For selected references see: (a) Danopoulos, A. A.; Braunstein, P.; Stylianides, N.; Wesolek, M. *Organometallics* **2011**, *30*, 6514−6517. (b) Liu, Y.; Luo, L.; Xiao, J.; Wang, L.; Song, Y.; Qu, J.; Luo, Y.; Deng, L. *Inorg. Chem.* **2015**, *54*, 4752−4760. (c) Ouyang, Z.; Deng, L. *Organometallics* **2013**, *32*, 7268−7271. (d) Hashimoto, T.; Urban, S.; Hoshino, R.; Ohki, Y.; Tatsumi, T.; Glorius, F. *Organometallics* **2012**, *31*, 4474−4479. (e) Przyojski, J. A.; Arman, H. D.; Tonzetich, Z. J. *Organometallics* **2012**, *31*, 3264−3271. (f) Wu, J.; Dai, W.; Farnaby, J. H.; Hazari, N.; Le Roy, J. J.; Mereacre, V.; Murugesu, M.; Powell, A. K.; Takase, M. K. *Dalton Trans* **2013**, *42*, 7404−7413.

(15) (a) Baillie, S. E.; Clegg, W.; García-Álvarez, P.; Hevia, E.; Kennedy, A. R.; Klett, J.; Russo, L. *Organometallics* **2012**, *31*, 5131−5142. (b) Armstrong, D. R.; Emerson, H. S.; Hernán-Gómez, A.; Kennedy, A. R.; Hevia, E. *Dalton Trans.* **2014**, *43*, 14229−14238.

(16) Recently, this cocomplexation method has also been applied to the synthesis of a range of divalent transition-metal HMDS-ate complexes (M = Mn, Fe, Co), including the solvent-free lithium ferrate $[LiFe(HMDS)_3]$; see ref 10g.

(17) (a) Andersen, R. A.; Faegri, K., Jr.; Green, J. C.; Haaland, A.; Lappert, M. F.; Leung, W. P.; Rypdal, K. *Inorg. Chem.* **1988**, *27*, 1782−1786. (b) $Fe(HMDS)_2$ exhibits a dimeric arrangement in the solid state with three-coordinate Fe centers; see: Olmstead, M. M.; Power, P. P.; Shoner, S. C. *Inorg. Chem.* **1991**, *30*, 2547−2551.

(18) Baillie, S. E.; Clegg, W.; García-Álvarez, P.; Hevia, E.; Kennedy, A. R.; Klett, J.; Russo, L. *Chem. Commun.* **2011**, *47*, 388−390.

(19) The same monomeric motif has been previously described for the solvent-free lithium magnesiate analogue $[LiMg(HMDS)_3]$; see: Kennedy, A. R.; Mulvey, R. E.; Rowlings, R. B. *J. Am. Chem. Soc.* **1998**, *120*, 7816−7824.

(20) (a) Armstrong, D. R.; Brammer, E.; Cadenbach, T.; Hevia, E.; Kennedy, A. R. *Organometallics* **2013**, *32*, 480−489. (b) Armstrong, D. R.; Herd, E.; Graham, D. V.; Hevia, E.; Kennedy, A. R.; Clegg, W.; Russo, L. *Dalton Trans.* **2008**, 1323−1330. (c) Francos, J.; Fleming, B. J.; García-Álvarez, P.; Kennedy, A. R.; Reilly, K.; Robertson, G. M.; Robertson, S. D.; O'Hara, C. T. *Dalton Trans.* **2014**, *43*, 14424−14431.

(21) For other examples of donor-free s-block tris(HMDS)-ate complexes see ref 19 and: Kennedy, A. R.; Mulvey, R. E.; Rowlings, R. B. *J. Organomet. Chem.* **2002**, *648*, 288−292.

(22) Margraf, G.; Schödel, F.; Sänger, I.; Bolte, M.; Wagner, M.; Lerner, H. W. *Z. Naturforsch.* **2012**, *67b*, 549−556.

(23) The sum of the internal angles around Fe in **1** is 359.97°, ranging from 110.48(10) to 124.93(10)°.

(24) Avent, A. G.; Antolini, F.; Hitchcock, P. B.; Khvostov, A. V.; Lappert, M. F.; Protchenko, A. V. *Dalton Trans.* **2006**, 919−927.

(25) An major deviation of these values is observed when **1** is compared with the solvent-free trimeric amide $[\{Na(HMDS)\}_3]$ (mean Na—N bond distance 2.381 Å; mean NNaN bond angle 139.7°); see: Driess, M.; Pritzkow, H.; Skipinski, M.; Winkler, U. *Organometallics* **1997**, *16*, 5108−5112.

(26) The concept of anchoring/ancillary bonding in heterobimetallic chemistry has previously been introduced in the literature by Mulvey; see: Mulvey, R. E. *Chem. Commun.* **2001**, 1049−1056.

(27) Kennedy, A. R.; Klett, J.; Mulvey, R. E.; Newton, S.; Wright, D. S. *Chem. Commun.* **2008**, 308−310.

(28) For other related examples of structural similarities in alkali-metal manganate and ferrate chemistry see refs 5a and 10g.

(29) This value compares well with those found in the monomeric sodium ferrate $[(TMEDA)NaFe(TMP)(CH_2SiMe_3)_2]$ (mean Fe—C bond length 2.086 Å) or iron(II) alkyl $[(TMEDA)Fe(CH_2SiMe_3)_2]$ (mean Fe—C bond length 2.078 Å); see ref 5c for details.

(30) Evans, D. F. *J. Chem. Soc.* **1959**, 2003−2005.

(31) This electronic configuration is in line with those reported in the literature for other trigonal-planar Fe(II) complexes; for selected references see: (a) Andres, H.; Bominaar, E. L.; Smith, J. M.; Eckert, N. A.; Holland, P. L.; Münck, E. *J. Am. Chem. Soc.* **2002**, *124*, 3012−3025. (b) Holland, P. L. *Acc. Chem. Res.* **2008**, *41*, 905−914. (c) Pugh, T.; Layfield, R. A. *Dalton Trans.* **2014**, *43*, 4251−4254. (d) Eichhöfer, A.; Lan, Y.; Mereacre, V.; Bodenstein, T.; Weigend, F. *Inorg. Chem.* **2014**, *53*, 1962−1974. (e) Fillman, K. L.; Przyojski, J. A.; Al-Afyouni, M. H.; Tonzetich, Z. J.; Neidig, M. L. *Chem. Sci.* **2015**, *6*, 1178−1188.

(32) This chemical shift appears in the same region as $SiMe_3$ resonances of $[\{(-)\text{-spartaine}\}Fe(CH_2SiMe_3)_2]$ (δ 10.14 and 15.71 ppm); see: Bart, S. C.; Hawrelak, E. J.; Schmisseur, A. K.; Lobkovsky, E.; Chirik, P. J. *Organometallics* **2004**, *23*, 237−246.

(33) Attempts to measure the solution magnetic moment of **2** using the Evans method proved unsuccessful, due to irreproducible chemical shift differences between the internal reference sample and residual protic solvent producing exceedingly large μ_{eff} values. The solution-phase effective moments of compounds **3**−**6** were determined by the Evans method. In all cases values were found that are consistent with a high-spin $S = 2$ electronic configuration; see the Supporting Information for details.

DOI: 10.1021/acs.inorgchem.5b01638
Inorg. Chem. 2015, 54, 9201−9210

(34) Hursthouse, M. B.; Rodesiler, P. F. *J. Chem. Soc., Dalton Trans.* **1972**, 2100−2102.
(35) Putzer, M. A.; Neumüller, B.; Dehnicke, K.; Magull, J. *Chem. Ber.* **1996**, *129*, 715−719.
(36) Hill, M. S.; Kociok-Köhn, G.; MacDougall, D. J. *Inorg. Chem.* **2011**, *50*, 5234−5241.
(37) Armstrong, D. R.; Baillie, S. E.; Blair, V. L.; Chabloz, N. G.; Diez, J.; Garcia-Alvarez, J.; Kennedy, A. R.; Robertson, S. D.; Hevia, E. *Chem. Sci.* **2013**, *4*, 4259−4266.
(38) For an insightful, up-to-date review on anionic (or ditopic) NHCs see: Waters, J. B.; Goicoechea, J. M. *Coord. Chem. Rev.* **2015**, *293*−*294*, 80−94.
(39) Layfield, R. A.; McDouall, J. J.; Scheer, M.; Schwarzmaier, C.; Tuna, F. *Chem. Commun.* **2011**, *47*, 10623−10625.
(40) Uzelac, M.; Hernan-Gomez, A.; Armstrong, D. R.; Kennedy, A. R.; Hevia, E. *Chem. Sci.* **2015**, DOI: 10.1039/C5SC02086G.
(41) Wang, Y.; Xie, Y.; Abraham, M. Y.; Wei, P.; Schaefer, H. F.; Schleyer, P. v R.; Robinson, G. H. *J. Am. Chem. Soc.* **2010**, *132*, 14370−14372.
(42) Day, B. M.; Pugh, T.; Hendriks, D.; Guerra, C. F.; Evans, D. J.; Bickelhaupt, F. M.; Layfield, R. A. *J. Am. Chem. Soc.* **2013**, *135*, 13338−13341.
(43) Significantly, on its own $Fe(HMDS)_2$ cannot metalate **IPr**. Instead, it forms the adduct $[(IPr)Fe(HMDS)_2]$; see ref 39.
(44) For a recent example of lateral lithiation of an NHC see: Danopoulos, A. A.; Braunstein, P.; Rezabalc, E.; Frison, G. *Chem. Commun.* **2015**, *51*, 3049−3052.
(45) El-Hellani, A.; Lavallo, V. *Angew. Chem., Int. Ed.* **2014**, *53*, 4489−4493.
(46) Arnold et al. have described the isolation of a bimetallic potassium/yttrium anionic N-heterocyclic dicarbene complex resulting from the reduction of an yttrium NHC complex with potassium naphthalenide, which is formally a deprotonation product: Arnold, P. L.; Liddle, S. T. *Organometallics* **2006**, *25*, 1485−1491.
(47) Musgrave, R. A.; Turbervill, R. S. P.; Irwin, M.; Herchel, R.; Goicoechea, J. M. *Dalton Trans.* **2014**, *43*, 4335−4344.
(48) (a) Wang, Y.; Xie, Y.; Abraham, M. Y.; Gilliard, R. J.; Wei, P.; Campana, C. F.; Schaefer, H. F.; Schleyer, P. v. R.; Robinson, G. H. *Angew. Chem., Int. Ed.* **2012**, *51*, 10173−10176. (b) Wang, Y.; Abraham, M. Y.; Gilliard, R. G., Jr.; Wei, P.; Smith, J. C.; Robinson, G. H. *Organometallics* **2012**, *31*, 791−796.
(49) (a) Arnold, P. L.; Pearson, S. *Coord. Chem. Rev.* **2007**, *251*, 596−609. (b) Schuster, O.; Yang, L.; Raubenheimer, H. G.; Albrecht, M. *Chem. Rev.* **2009**, *109*, 3445−3478. (c) Crabtree, R. H. *Coord. Chem. Rev.* **2013**, *257*, 755−766.
(50) See refs 31d and 42 and: (a) Danopoulos, A. A.; Tsoureas, N.; Wright, J. A.; Light, M. E. *Organometallics* **2004**, *23*, 166−168. (b) Lavallo, V.; El-Batta, A.; Bertrand, G.; Grubbs, R. H. *Angew. Chem., Int. Ed.* **2011**, *50*, 268−271.
(51) Aldeco-Perez, E.; Rosenthal, A. J.; Donnadieu, B.; Parameswaran, P.; Frenking, G.; Bertrand, G. *Science* **2009**, *326*, 556−559.
(52) Chilton, N. F.; Anderson, R. P.; Turner, L. D.; Soncini, A.; Murray, K. S. *J. Comput. Chem.* **2013**, *34*, 1164−1175.
(53) Boča, R. *Coord. Chem. Rev.* **2004**, *248*, 757−815.
(54) Bendix, J.; Brorson, M.; Schäffer, C. E. *Inorg. Chem.* **1993**, *32*, 2838−2849.
(55) Lin, P.-H.; Smythe, N. C.; Gorelsky, S. I.; Maguire, S.; Henson, N. J.; Korobkov, I.; Scott, B. L.; Gordon, J- C.; Baker, R. T.; Murugesu, M. *J. Am. Chem. Soc.* **2011**, *133*, 15806−15809.
(56) Goswami, T.; Misra, A. *J. Phys. Chem. A* **2012**, *116*, 5207−5215.

DOI: 10.1021/acs.inorgchem.5b01638
Inorg. Chem. 2015, 54, 9201−9210